

The solid-state thermal rearrangement of the Dawson anion $[P_2Mo_{18}O_{62}]^{6-}$ into a Keggin-type $[PMo_{12}O_{40}]^{3-}$ -containing phase and their reactivity in the oxidative dehydrogenation of isobutyraldehyde

Ji Hu ^a, Robert C. Burns ^{a,*}, Jean-Pierre Guerbois ^b

^a Department of Chemistry, The University of Newcastle, Callaghan 2308, New South Wales, Australia

^b Department of Chemistry, Materials and Forensic Science, University of Technology, Sydney 2007, Australia

Received 9 February 1999; accepted 17 June 1999

Abstract

The thermal and structural stability of the Dawson-type heteropolyoxometalate anion, $[P_2Mo_{18}O_{62}]^{6-}$, with varying counter cations $[K^+, Rb^+, Cs^+, NH_4^+]$ and $(CH_3)_4N^+$ and water/solvent (1,4-dioxane) of crystallization has been examined using IR spectroscopy, XRD, TGA/DTA, TEM/SEM and ^{31}P solid-state NMR spectroscopy. At temperatures higher than about 260°C, the K^+ , Rb^+ and Cs^+ salts undergo an irreversible thermal rearrangement to give the corresponding Keggin anion $[PMo_{12}O_{40}]^{3-}$ as one product, along with a second phase which appears to be another phosphorous-containing polyoxomolybdate, perhaps $[P_2Mo_6O_{26}]^{6-}$ or a mixture of related species. Although the NH_4^+ and Me_4N^+ salts behave similarly, the second phase does not seem to be as thermally stable in these systems, and at higher temperatures, decomposition to MoO_3 is observed. Gas-phase oxidative dehydrogenation of isobutyraldehyde to methacrolein was used to examine the effectiveness of the $[P_2Mo_{18}O_{62}]^{6-}$ salts and their thermally-rearranged phases as catalysts. The former are poor catalysts, undergoing thermal rearrangement even at 250°C under catalytic conditions, which is related to the role of the catalyst in the reaction. The thermally-rearranged NH_4^+ and Me_4N^+ salts are highly active catalysts at 300°C, even resulting in the formation of some methacrylic acid, while the thermally-rearranged phases in the K^+ , Rb^+ and Cs^+ systems show little activity. The latter likely results from the presence of the catalytically-inactive second phase(s) formed in the thermal rearrangement in each case, which forms a surface layer on the catalytically-active $[PMo_{12}O_{40}]^{3-}$ phase. © 2000 Elsevier Science B.V. All rights reserved.

Keywords: Isobutyraldehyde; Dawson; Keggin; Oxidative dehydrogenation; Thermal rearrangement

1. Introduction

Heteropolyoxometalate acids and salts have been shown to be highly effective heterogeneous catalysts for the gas-phase selective oxidation of organic substrates, such as the oxida-

* Corresponding author. Tel.: +61-2-49215479; E-mail: crrb@paracelsus.newcastle.edu.au

tive dehydrogenation of isobutyric acid and the oxidation of methacrolein, both of which yield methacrylic acid [1–5]. They are also useful acid catalysts, and processes based on their redox and acid–base properties are used industrially [3–5]. The study of heteropolyoxometalates as oxidation–reduction catalysts has involved primarily Keggin-based structures, particularly $[\text{PMo}_{12}\text{O}_{40}]^{3-}$, and substituted species involving replacement of one or more framework Mo(VI) by V(V) [4,5]. The geometry of the $(\alpha\text{-})[\text{PMo}_{12}\text{O}_{40}]^{3-}$ ion consists of a central tetrahedrally coordinated phosphorus atom surrounded by four groups of three edge-sharing octahedra (i.e., Mo_3O_{13} subunits), which are in turn linked to each other and to the central PO_4 tetrahedron by shared oxygen atoms at the vertices [6].

Recently, attention has turned to the use of heteropoly species that exhibit the Dawson structure in gas-phase heterogeneous catalytic systems. This latter structure is based on the Keggin geometry but has three MO_3 ($\text{M} = \text{Mo}$ or W) groups removed, one each from three adjacent M_3O_{13} subunits, with two such resulting “ $[\text{PM}_9\text{O}_{31}]^{3-}$ ” units joined to produce the dimeric $[\text{P}_2\text{M}_{18}\text{O}_{62}]^{6-}$ Dawson-type anion ($\text{M} = \text{Mo}$ or W). On the basis of solution electrochemical studies, the Dawson-structure species are slightly stronger oxidants than their related Keggin-structure counterparts [6], suggesting that they may exhibit similar or even better performance in gas-phase heterogeneous catalytic oxidation or oxidative dehydrogenation reactions.

Substituted Dawson-type anions of formula $\text{K}_x[\text{P}_2\text{W}_{17}\text{MO}_{62-y}] \cdot n\text{H}_2\text{O}$, where $y = 0$ when $\text{M} = \text{W(VI)}$ and $y = 1$ when $\text{M} = \text{Fe(III)}$, Mn(III) , Co(II) or Cu(II) , have been used for the oxidative dehydrogenation of isobutane to isobutene [7]. In a similar study, the solid-state thermal rearrangement of $\text{K}_6[\text{P}_2\text{W}_{18}\text{O}_{62}] \cdot 10\text{H}_2\text{O}$ was examined, which led to a stable Keggin heteropolyanion phase, as well as the use of this phase in the oxidation of isobutane to isobutene [8]. The thermal rearrangement

was observed to occur at $\sim 527^\circ\text{C}$, yielding $\text{K}_3[\text{PW}_{12}\text{O}_{40}]$ and an additional phase, which was in turn formed from the high temperature interaction of K_3PO_4 , also assumed to have resulted from the decomposition of $\text{K}_6\text{P}_2\text{W}_{18}\text{O}_{62} \cdot 10\text{H}_2\text{O}$, and the product Keggin phase itself. The resulting material exhibited higher activity towards the oxidative dehydrogenation of isobutane to isobutene than both the original Dawson compound and a pure $\text{K}_3[\text{PW}_{12}\text{O}_{40}]$ catalyst. This was attributed to the presence of an amorphous surface layer, of unknown stoichiometry, on the thermally-formed Keggin compound. To date, however, there have been no reports dealing with the thermal stability of the related Dawson-type $[\text{P}_2\text{Mo}_{18}\text{O}_{62}]^{6-}$ ion and its use in the selective oxidative dehydrogenation or oxidation of organic substrates such as isobutyric acid or methacrolein. In this study, the thermal and structural stability of various salts [with K^+ , Rb^+ , Cs^+ , NH_4^+ and $(\text{CH}_3)_4\text{N}^+$ counter cations] of the $[\text{P}_2\text{Mo}_{18}\text{O}_{62}]^{6-}$ ion are examined, and their application in a typical oxidative dehydrogenation reaction, in this case the selective conversion of isobutyraldehyde to methacrolein in the gas-phase, are investigated. The oxidative dehydrogenation of isobutyraldehyde offers an alternative route to the formation of methacrolein, oxidation of which yields methacrylic acid, which upon esterification yields methyl methacrylate and ultimately methyl methacrylate polymers. Isobutyraldehyde is obtained as a product by the hydroformylation of propene. The oxidative dehydrogenation of isobutyraldehyde over numerous catalysts has been studied, such as iron phosphate [9], as well as phosphomolybdic acid containing Sb, Zn and Cr (88.3% conversion at 295°C ; 40.8 and 6.9% methacrolein and methacrylic acid, respectively) [10] and Zr, V and Cs (100% conversion at 310°C ; 76.5 and 8.9% methacrolein and methacrylic acid) [11]. In the present study, comparisons of salts of the $[\text{P}_2\text{Mo}_{18}\text{O}_{62}]^{6-}$ ion are made with thermally-rearranged phases that are formed at higher temperatures and also with pure Keggin salts containing selected cations.

2. Experimental

2.1. Preparation and characterization of salts of the $[P_2Mo_{18}O_{62}]^{6-}$ and $[PMo_{12}O_{40}]^{3-}$ anions

The $[P_2Mo_{18}O_{62}]^{6-}$ anion was prepared using the method described by Tsigidinos [12], by refluxing an acidic (HCl) aqueous solution of Na_2MoO_4 and phosphoric acid for 8 h. The K^+ , Rb^+ , Cs^+ , NH_4^+ and Me_4N^+ salts were obtained by addition of a slight excess of their respective chlorides to an aqueous 1,4-dioxane (50:50% v/v) solution of the $[P_2Mo_{18}O_{62}]^{6-}$ ion, as prepared above, and in each case, yielded a bright yellow solid. The K^+ and NH_4^+ salts were easily recrystallized from a H_2O /dioxane (1:1) solution. Thermogravimetric and chemical analysis showed that all compounds contained variable amounts of non-structural water, which was easily lost on storage and, with the exception of the Me_4N^+ salt, also contained dioxane. The infrared spectra of all compounds in the metal–oxygen stretching range (i.e., 1200–600 cm^{-1}) were almost identical, and were also identical with that of $[(n - C_4H_9)_4N]_5-H[P_2Mo_{18}O_{62}]$, which has been reported by Garvey and Pope [13]. Cyclic voltammetry of the NH_4^+ salt (1×10^{-3} M) in 0.5 M H_2SO_4 /1,4-dioxane (1:1) solution, exhibited four reversible 2-electron couples with half-wave potentials of +0.338, +0.216, –0.016 and –0.288 V vs. a Ag/AgCl electrode, in agreement with published data [14]. The ^{31}P NMR spectra of the K^+ , Rb^+ , Cs^+ and NH_4^+ salts in D_2O and the Me_4N^+ salt in dimethyl sulfoxide exhibited single resonances at $\delta = -2.22$, –2.26, –2.28, –2.26 and –2.18 ppm, respectively, relative to 85% H_3PO_4 , indicating the absence of any impurities.

The K^+ and Me_4N^+ salts of the $[PMo_{12}O_{40}]^{3-}$ ion were prepared by addition of a stoichiometric amount of K_2CO_3 and $Me_4N^+Cl^-$ to concentrated aqueous solutions of $H_3[PMo_{12}O_{40}] \cdot 23H_2O$ (water content determined by TGA) and isolating the yellow products by filtration, washing and drying at room

temperature. The compound $(NH_4)_3[PMo_{12}O_{40}]$ was obtained commercially (Aldrich). The infrared spectra of all three compounds and the ^{31}P NMR spectrum of the Me_4N^+ salt ($\delta = -2.73$ ppm from 85% H_3PO_4 ; in DMSO solvent) were in agreement with published data [15,16].

Thermogravimetric and differential thermal analyses (TGA/DTA) were performed on a TA Instruments SDT 2960 Simultaneous DTA-TGA or, for the former, on a Stanton Redcroft TG-750 instrument coupled to a Eurotherm Model 94 temperature controller. Sample masses of about 10 mg were used with a heating rate of 5 or 10°C/min in an air atmosphere, and at a flow rate of 10 ml/min. Infrared (IR) spectra were recorded on a Bio-Rad FTS-7 Fourier-transform spectrophotometer, with samples mounted as KBr discs. X-ray powder diffraction (XRD) was performed on a Philips PW1700 Automated Powder Diffractometer System 1, employing graphite-monochromated $Cu-K_{\alpha}$ radiation. Transmission electron micrographs (TEM) were recorded using a Jeol 1200-EXII transmission microscope operating at 80 kV. Samples were prepared by dispersing the crystals in chloroform, 1,1,1-trichloroethane or Millipore Milli-Q water using an ultrasonic treatment and evaporating to dryness on a copper-supported carbon film. Scanning electron microscopy (SEM) was performed on a Philips XL-30 scanning electron microscope operating at 15 kV. Cyclic voltammetric studies were conducted on a PAR Model 273A Potentiostat/Galvanostat using a standard three-electrode system, which consisted of a glassy carbon working electrode, an auxiliary platinum electrode and an aqueous Ag/AgCl reference electrode. Solution ^{31}P NMR spectra were obtained with a Bruker AVANCE DPX-300 spectrometer operating at 121.49 MHz, while the solid-state ^{31}P NMR spectra were obtained with a Bruker MAS-300 spectrometer operating at 121.49 MHz. The reference used was external 85% H_3PO_4 for the solution spectra and $(NH_4)H_2PO_4$ for the solid-state spectra. For the solid-state spectra samples (~ 150 mg)

were contained in a partially-stabilized zirconia tube fitted with a Kel-F cap, and were spun at 10 kHz. Surface area measurements were made by the BET method using nitrogen adsorption on a Micromeritics ASAP 2400 instrument.

2.2. Catalysis and analysis of products

The catalytic activities of the various salts of the $[P_2Mo_{18}O_{62}]^{6-}$ and $[PMo_{12}O_{40}]^{3-}$ ions, and of selected thermally-rearranged phases formed from the former on heating to 310 or 550°C, towards the gas-phase oxidative dehydrogenation of isobutyraldehyde were carried out using a conventional flow fixed-bed reactor (a 30 cm long quartz tube with an internal diameter of 4 mm). Reactions were conducted at atmospheric pressure and at temperatures of 225, 250, 275 and 300°C. The feed gas consisted of 1% isobutyraldehyde (Aldrich, 98%, freshly distilled under nitrogen and transferred to the catalysis system saturator using a gas-tight syringe) and 3% oxygen, with a nitrogen balance. The saturator was held at 0°C using an ethanol–water cold bath. For the Dawson phases and the thermally-rearranged phases, a catalyst mass of 0.50 g (~0.35 ml) was used for each study (after allowing for loss of water and/or dioxane), which when combined with a flow rate of 150 ml/min gave a residence time of 0.14 s assuming plug flow. This corresponds to a W/F (weight of catalyst per total flow rate) of 0.2 g s/ml. For studies of the selected Keggin phases, a catalyst mass of 0.20 g (~0.13 ml) was used, giving a residence time of 0.05 s under the same conditions, and a W/F of 0.08 g s/ml. All catalysts were prepared by compressing powdered samples at a pressure of 1.7 ton/cm², broken up and passed through a series of sieves, with the fraction from 40 to 80 mesh used for the actual catalysis. The catalyst samples were loaded between silica wool plugs in the quartz reactor tube. Samples were calcined at various temperatures as described below for 2 h under a flow of nitrogen + 3% oxygen prior to catalytic investigation.

Following the establishment of a steady state in each case (~4 h), which was monitored by the IR detection and analysis of both CO and CO₂, the condensable gaseous products, that is methacrolein, acetone and methacrylic acid, as well as unreacted isobutyraldehyde, were collected in an acetone–dry ice cold bath for a period of 30 min, and used as representative of the conversion and selectivity for the sampling time. The water produced during the reaction was not determined. The above products were analysed by gas chromatography (3 wt.% FFAP and 7 wt.% OV-17 on Chromosorb-W). The carbon balance was routinely in the range 90–100%. The conversion of isobutyraldehyde was calculated as $100[1 - (\text{moles of unreacted isobutyraldehyde} / \text{moles of isobutyraldehyde introduced})]$, while the selectivities of the various products were determined as $100(\text{moles of component } i / \text{total number of moles of products})$.

2.3. Extended-Hückel molecular orbital calculations

Extended-Hückel molecular orbital calculations were performed using the package described by Mealli and Proserpio [17] (Version 4.0, 1994), with the extended-Hückel parameters, i.e., Coulomb integrals, H_{ii} (eV) and Slater exponents (ξ), taken from the values provided in the package. The Wolfsberg–Helmholtz constant was set to 1.75. For the phosphorus-containing heteropolyoxomolybdate anions, the X-ray crystallographic coordinates for both $Na_6[P_2Mo_{18}O_{62}] \cdot 24H_2O$ [18] and $H_3[PMo_{12}O_{40}] \cdot 30H_2O$ [19,20] were used for all anion atoms, while a P–O distance of 1.537 Å was used for the PO_4^{3-} ion [21].

3. Results and discussion

3.1. Thermal decomposition of compounds containing the $[P_2Mo_{18}O_{62}]^{6-}$ ion

A series of compounds of the $[P_2Mo_{18}O_{62}]^{6-}$ ion with K^+ , Rb^+ , Cs^+ , NH_4^+ and Me_4N^+ as

the cations were heated to different temperatures for 4 h and the resulting products examined by IR spectroscopy and XRD. The 4-h timeframe was chosen as it has been shown in previous studies that at least this length of time is required for a heteropolyoxomolybdate catalyst containing the $[\text{PMo}_{12}\text{O}_{40}]^{3-}$ ion to reach a steady state in a typical oxidative dehydrogenation reaction such as, for example, the conversion of isobutyric acid to methacrylic acid [2] or isobutyraldehyde to methacrolein [22]. The data for the K^+ and NH_4^+ compounds are shown in Figs. 1–4, along with the IR spectra and XRD patterns of the corresponding $[\text{PMo}_{12}\text{O}_{40}]^{3-}$ compounds. It is apparent that $[\text{P}_2\text{Mo}_{18}\text{O}_{62}]^{6-}$ undergoes a thermal rearrangement above $\sim 260^\circ\text{C}$ to give the Keggin-type ion $[\text{PMo}_{12}\text{O}_{40}]^{3-}$ as one product. The IR spectra of the K^+ and NH_4^+ compounds (Figs. 1 and 2, respectively) indicate that almost no decomposition occurs at 255°C after 4 h, while the XRD studies (Figs. 3 and 4, respectively) show that at 270°C rearrangement takes place over this period of time. At 310°C both $\text{K}_3[\text{PMo}_{12}\text{O}_{40}]$ and $(\text{NH}_4)_3[\text{PMo}_{12}\text{O}_{40}]$ are thermally stable, with the former remaining stable up to at least 700°C while the latter decomposes to MoO_3 (molybdate) by 550°C . The behaviour of the Rb^+ and Cs^+ compounds is almost identical to that of the K^+ salt. The Me_4N^+ salt shows some rearrangement after 4 h at 270°C , but apparently less conversion than the other compounds, formation of a partial Keggin structure at 310°C and decomposition to MoO_3 by 550°C .

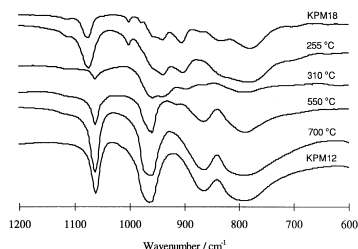


Fig. 1. Infrared spectra of $\text{K}_6\text{P}_2\text{Mo}_{18}\text{O}_{62}$ (KPM18), of samples treated in air at 255, 310, 550, and 700°C for 4 h, and of $\text{K}_3\text{PMo}_{12}\text{O}_{40}$ (KPM12).

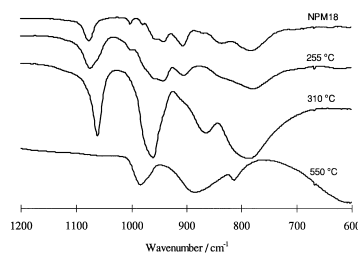


Fig. 2. IR spectra of $(\text{NH}_4)_6\text{P}_2\text{Mo}_{18}\text{O}_{62}$ (NPM18), of samples treated in air at 255, 310 and 550°C for 4 h. The latter is identical with that of MoO_3 over the same wavenumber range.

For the K^+ , Rb^+ , Cs^+ and NH_4^+ compounds, all of which were prepared with considerable 1,4-dioxane and water in their structures, TGA/DTA studies indicate that dioxane and/or water are lost in various overlapping stages, with constant mass only being obtained above 500°C . In the case of the NH_4^+ compound, this also involves decomposition of the cation, probably initially into NH_3 and H^+ , followed by decomposition of the acid (to P_2O_5 and MoO_3). A typical TGA/DTA study of the freshly crystallized K^+ salt, $\text{K}_6[\text{P}_2\text{Mo}_{18}\text{O}_{62}] \cdot 4\text{C}_4\text{H}_8\text{O}_2 \cdot 16\text{H}_2\text{O}$, is shown in Fig. 5. Weakly adsorbed and bound water and/or dioxane appears to be lost continually up to $\sim 250^\circ\text{C}$, with a major loss in mass associated with an exothermic reaction occurring above this temperature (270°C). The results for the Rb^+ and NH_4^+ compounds are similar, with the first major exothermic reactions occurring at 274 and 277°C , respectively, while the Cs^+ compound has two strongly exothermic peaks at 248 and 273°C . The data for $(\text{Me}_4\text{N})_6[\text{P}_2\text{Mo}_{18}\text{O}_{62}] \cdot 3\text{H}_2\text{O}$ are somewhat

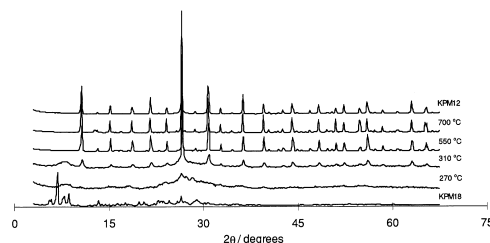


Fig. 3. XRD patterns of $\text{K}_6\text{P}_2\text{Mo}_{18}\text{O}_{62}$ (KPM18), of samples treated in air at 270, 310, 550, and 700°C for 4 h, and of $\text{K}_3\text{PMo}_{12}\text{O}_{40}$ (KPM12).

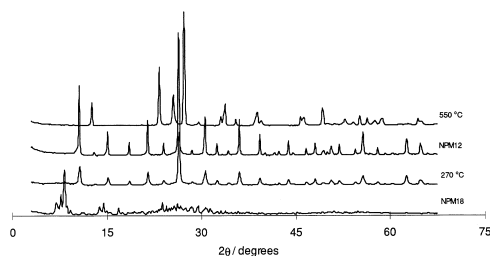


Fig. 4. XRD patterns of $(\text{NH}_4)_6\text{P}_2\text{Mo}_{18}\text{O}_{62}$ (NPM18), of samples treated in air at 270 and 550°C for 4 h, and of $(\text{NH}_4)_3\text{PMo}_{12}\text{O}_{40}$ (NPM12). The XRD pattern of the sample heated to 550°C is identical with that of MoO_3 .

different, with an initial mass loss from room temperature to about 140°C associated with loss of the $3\text{H}_2\text{O}$ in the lattice, followed by two main exothermic mass losses at 300–360°C and 360–480°C. The latter are associated with decomposition of the Me_4N^+ ions, probably as Me_3N , ethene and water. To higher temperatures, all samples, irrespective of the cation, continually lost mass above $\sim 700^\circ\text{C}$ as a result of the volatilization of MoO_3 .

The significant mass losses associated with the exothermic peaks at $\sim 270^\circ\text{C}$ for the K^+ , Rb^+ , Cs^+ and NH_4^+ compounds may be associated with the loss of dioxane and/or water, and perhaps with the thermal rearrangement of the $[\text{P}_2\text{Mo}_{18}\text{O}_{62}]^{6-}$ ion into the $[\text{PMo}_{12}\text{O}_{40}]^{3-}$ ion. Indeed, the thermal rearrangement of the Dawson anion may trigger the significant loss of dioxane and/or water from the structures. However, examination of the TGA/DTA results for $(\text{Me}_4\text{N})_6[\text{P}_2\text{Mo}_{18}\text{O}_{62}] \cdot 3\text{H}_2\text{O}$ shows no evidence for an exothermic peak at or close to this temperature. This is in contrast to the related compound $\text{K}_6[\text{P}_2\text{W}_{18}\text{O}_{62}] \cdot 10\text{H}_2\text{O}$, which is reported to undergo an exothermic reaction at 527°C , with no associated mass loss, and therefore, attributable to a thermal rearrangement [8]. The nearest exothermic peak for the Me_4N^+ salt in the present study was found at 363°C , but this is associated with a mass loss of some 3%. It should be pointed out that the timescales of the TGA/DTA study and the IR spectroscopic

and XRD studies were somewhat different, and that thermal rearrangement of $[\text{P}_2\text{Mo}_{18}\text{O}_{62}]^{6-}$ at a static temperature of $\sim 260^\circ\text{C}$ is relatively slow. This is demonstrated by the slow thermal rearrangement of the Me_4N^+ salt at 270°C , as noted above, and is the likely reason for lack of an exothermic peak appearing in the TGA/DTA trace at or around this temperature. Moreover, the thermal rearrangement appears to depend on the extent of inclusion of dioxane and water into the structure, and on its ease of removal. In the case of the K^+ , Rb^+ , Cs^+ and NH_4^+ compounds, all of which contain significant quantities of dioxane and/or water, facile loss of some of these likely results in a relatively open structure, allowing diffusion of mobile components and hence an easy pathway to the formation of the products. This is supported by the effectively amorphous nature of the solid during thermal rearrangement (see Fig. 3, 270°C). However, for the Me_4N^+ salt only three H_2O molecules per $(\text{Me}_4\text{N})_6[\text{P}_2\text{Mo}_{18}\text{O}_{62}]$ are included in the structure and, although they are lost by $\sim 140^\circ\text{C}$, the $3\text{H}_2\text{O}$ have only a small relative volume in the structure, perhaps leading to a less open structural framework during rearrangement and hence to a more constricted and slower thermal rearrangement at $260\text{--}270^\circ\text{C}$.

As proposed in the study of the thermal stability of $\text{K}_6[\text{P}_2\text{W}_{18}\text{O}_{62}] \cdot 10\text{H}_2\text{O}$ [8], the rear-

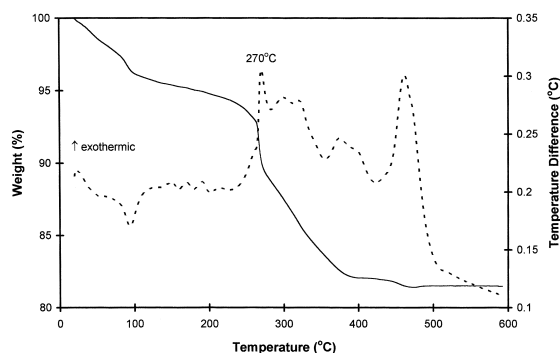
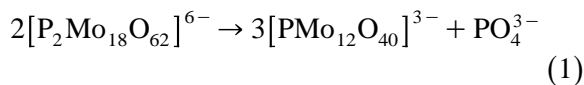


Fig. 5. TGA–DTA of $\text{K}_6[\text{P}_2\text{Mo}_{18}\text{O}_{62}] \cdot 4\text{C}_4\text{H}_8\text{O}_2 \cdot 16\text{H}_2\text{O}$ from room temperature to 600°C (heating rate, $10^\circ\text{C}/\text{min}$; air atmosphere, flow rate = $10 \text{ ml}/\text{min}$).

rangement of a Dawson anion can be represented by Eq. (1):



For this equation, the change in total stabilization energy $\Delta E_T = 3E_T(\text{PMo}_{12}\text{O}_{40}^{3-}) + E_T(\text{PO}_4^{3-}) - 2E_T(\text{P}_2\text{Mo}_{18}\text{O}_{62}^{6-})$, where E_T for a particular species, is the sum of the one-electron energies as calculated using the extended-Hückel molecular orbital (EHMO) approach, is equal to $3(-6288.9) + (-634.8) - 2(-9754.4) = +7.3$ eV. It should be noted that no cation–anion interactions have been allowed for in this calculation, and it is assumed that these are comparable for the reactant and product species. In view of the approximations inherent in the EHMO method, the actual value is not important except to indicate that the products are energetically less favoured than the original $[\text{P}_2\text{Mo}_{18}\text{O}_{62}]^{6-}$ ion, and that the relatively small value for ΔE_T compared to the individual E_T values for the reactant and product species is consistent with the ready thermal decomposition of $[\text{P}_2\text{Mo}_{18}\text{O}_{62}]^{6-}$ above room temperature. The equation, therefore, offers a reasonable description for the thermal decomposition of $[\text{P}_2\text{Mo}_{18}\text{O}_{62}]^{6-}$. The equation also suggests that a second component should be detectable as a result of the thermal decomposition and rearrangement process. Examination of the IR spectra and XRD patterns of the compounds following thermal rearrangement provides evidence for this second component.

The IR spectra of the K^+ and Rb^+ compounds following thermal decomposition at 550°C both show a weak shoulder at ~ 1125 cm^{-1} (see Fig. 1 for the K^+ salt), with evidence for several weak peaks to lower frequencies (~ 1015 , 912 and 750 – 650 cm^{-1}), while the Cs^+ compound exhibits extra peaks at 1175 , 940 and 895 cm^{-1} , with evidence for a broad absorption from 750 to 650 cm^{-1} . The data may be compared with that of $\text{K}_6[\text{P}_2\text{W}_{18}\text{O}_{62}] \cdot 10\text{H}_2\text{O}$

following thermal rearrangement at 800°C , which occur at 1203 , 1143 [both assigned as $\nu(\text{P}=\text{O})$] and 945 cm^{-1} , along with several broad bands in the $\nu(\text{W}=\text{O}=\text{W})$ region [8]. For the K^+ , Rb^+ and Cs^+ compounds of $[\text{P}_2\text{Mo}_{18}\text{O}_{62}]^{6-}$ following thermal rearrangement of the anion, the peaks at ~ 1125 and 1175 cm^{-1} may be assigned as $\nu(\text{P}=\text{O})$ stretching vibrations, while those at ~ 1015 , 940 , 912 and 895 cm^{-1} may also involve $\text{P}=\text{O}$ stretching [the Raman-active symmetric ν_1 mode for tetrahedral PO_4^{3-} occurs at 938 cm^{-1}], although they could also be attributed to $\nu(\text{Mo}=\text{O}=\text{Mo})$ stretching vibrations. The broad feature at 750 – 650 cm^{-1} in all compounds is attributable to several overlapping $\nu(\text{Mo}=\text{O}=\text{Mo})$ vibrations. The differences between the Cs^+ and other compounds suggests that the cation plays some role in the formation of the second component, with Cs^+ inhibiting its formation (see below). This could simply be related to the relative size of the Cs^+ cation.

Examination of the resulting XRD patterns of the K^+ , Rb^+ , Cs^+ and NH_4^+ -containing phases following thermal rearrangement of their precursor $[\text{P}_2\text{Mo}_{18}\text{O}_{62}]^{6-}$ compounds at different temperatures indicates that all major reflections can be indexed, using a Rietvelt profile analysis, on the basis of a cubic unit cell (space group $Pn3m$) with $a = 11.5921(2)$, $11.6710(2)$, $11.8195(3)$ and $11.688(1)$ Å ($Z = 2$), respectively. These agree closely with those of their corresponding Keggin structures (C^+) $_3[\text{PMo}_{12}\text{O}_{40}]$ ($\text{C}^+ = \text{K}^+$, Rb^+ , Cs^+ and NH_4^+) [22]. The Keggin structures are isomorphous and isostructural although there are, as expected, differences in the relative intensities of the peaks. The Keggin structures with K^+ , Rb^+ and Cs^+ counter cations are stable up to 700°C , although above this temperature, mass is lost through volatilization of MoO_3 , as noted above. Closer examination of the XRD patterns following heating for 4 h at different temperatures reveals that in the case of the K^+ , Rb^+ and Cs^+ compounds, there are several weak reflections which are present at 310°C , are less evident at 550°C and which have almost disappeared by

700°C. These also provide evidence of the presence of a second component given the time and temperatures of heating. The second phase thus appears to become effectively amorphous or perhaps glass-like at high temperatures for these three cation systems. Evidence for this is discussed below.

In order to test if the second phase could be synthesized by direct reaction, various mole ratios of $\text{K}_3\text{PMo}_{12}\text{O}_{40}$ and K_3PO_4 were heated to elevated temperatures in a platinum crucible. Reaction appeared very slow at 300°C, but at higher temperatures ($\sim 500^\circ\text{C}$) $\text{K}_3[\text{PMo}_{12}\text{O}_{40}]$ and K_3PO_4 reacted in the solid state [using well-ground and pressed discs ($5.7 \text{ ton}/\text{cm}^2$)] in less than 1 h. At a mole ratio for $\text{K}_3[\text{PMo}_{12}\text{O}_{40}]$ to K_3PO_4 of 1:3 the yellow colour was completely discharged, yielding a colourless product which melted at $\sim 525^\circ\text{C}$. This material showed IR absorptions at 1154s, 1107s, 1046s, 995m, 902vs and 690s cm^{-1} . Several of these correspond to the IR absorptions observed for the product of the thermal rearrangement of $\text{K}_6[\text{P}_2\text{Mo}_{18}\text{O}_{62}]$. Prior to fusion the IR spectrum exhibited a more complex spectrum, with many similar peaks as well as a strong absorption at 1183 cm^{-1} , which is reminiscent of the high frequency peak that was observed in the IR spectrum of thermally-rearranged $\text{Cs}_6[\text{P}_2\text{Mo}_{18}\text{O}_{62}]$. All of these absorptions have similar assignments to those given above. Based on the 1:3 mole ratio, this solid can be formulated as “ $\text{K}_6\text{P}_2\text{Mo}_6\text{O}_{26}$ ”. XRD examination of this material indicated that it was amorphous, even when a slow cooling rate was employed during solidification. It is thus likely to be a mixture of related species. Although the $[\text{P}_2\text{Mo}_6\text{O}_{26}]^{6-}$ ion is not presently known, the related $[\text{P}_2\text{Mo}_5\text{O}_{23}]^{6-}$ has been structurally characterized, along with the arsenic-containing species $[\text{As}_2\text{Mo}_6\text{O}_{26}]^{6-}$, which is a direct analogue of the proposed $[\text{P}_2\text{Mo}_6\text{O}_{26}]^{6-}$ ion. Importantly, both of the above species are colourless [6], as is the product of the reaction between $\text{K}_3[\text{PMo}_{12}\text{O}_{40}]$ and K_3PO_4 in a 1:3 mole ratio. The $[\text{As}_2\text{Mo}_6\text{O}_{26}]^{6-}$ ion consists of a ring of

six edge-shared MoO_6 octahedra, with capping AsO_4 tetrahedra above and below the ring. The $[\text{P}_2\text{Mo}_5\text{O}_{23}]^{6-}$ ion is similar, except that the ring is irregular and consists of five edge- and corner-shared MoO_6 octahedra [6]. As the Dawson structure is broken down during thermal rearrangement, it is likely that these or related species are formed in the process, in addition to $[\text{PMo}_{12}\text{O}_{40}]^{3-}$ ions. They are, however, not expected to be catalytically active as they contain *cis*-dioxo MoO_2 groups, which places limits on their reducibility and their use in catalytic reactions that require the facile formation of reduced heteropolyoxometalates [23].

TEM of $\text{K}_6[\text{P}_2\text{Mo}_{18}\text{O}_{62}] \cdot 4\text{C}_4\text{H}_8\text{O}_2 \cdot 16\text{H}_2\text{O}$ as prepared and after heating to various temperatures are shown in Fig. 6a–d. The freshly prepared compound (Fig. 6a) appeared to show several plate-like crystal forms, which is not surprising given the amount of 1,4-dioxane and water crystallized in the structure and the ready loss of the latter. On heating to 255°C the material consisted of agglomerates of small plate crystals (Fig. 6b). At 310°C , two crystal forms

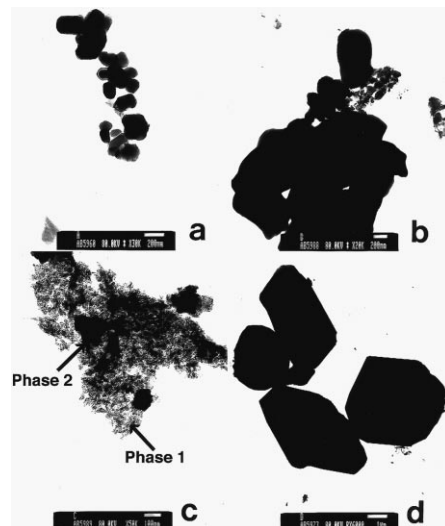


Fig. 6. TEM of $\text{K}_6[\text{P}_2\text{Mo}_{18}\text{O}_{62}] \cdot 4\text{C}_4\text{H}_8\text{O}_2 \cdot 16\text{H}_2\text{O}$: (a) freshly prepared at room temperature, (b), (c) and (d) heating at 255, 310 and 550°C for 4 h in air, respectively. The scale is given by the bar [(a) and (b) 200 nm, (c) 100 nm and (d) $1 \mu\text{m}$], just to the right of centre at the base of each micrograph.

could be observed. These included small acicular crystals (phase 1) and another poorly crystalline phase (phase 2) (Fig. 6c). The poorly crystalline phase was by far the most abundant and is certainly $K_3[PMo_{12}O_{40}]$. On heating to 550°C for 4 h, the resulting crystalline mass was no longer friable and exhibited considerable sintering. One major crystalline form was evident and, moreover, the crystals were considerably larger ($0.5\text{--}5\ \mu\text{m}$) than any observed in the sample heated to 310°C . The crystals exhibited a cubic or truncated cubic morphology (Fig. 6d; see also Fig. 7), and were similar to an authentic sample of $K_3[PMo_{12}O_{40}]$. SEM images of the sample treated at 550°C (Fig. 7) showed agglomerates of these crystals, which were covered by an amorphous surface coating (appearing at the top in Fig. 7), presumably, the result of reaction of the second component of the thermal breakdown of $K_6[P_2Mo_{18}O_{62}]$ with $K_3[PMo_{12}O_{40}]$. Notably, the product of the reaction of $K_3[PMo_{12}O_{40}]$ and K_3PO_4 in a 1:3 mole ratio was also amorphous, which is consistent with the formation of the coating in the sample calcined at 550°C , as observed in the SEM image.

Solid-state ^{31}P NMR studies, including those following thermal treatment of various samples, are shown in Fig. 8a–f, and provide



Fig. 7. SEM image of $K_6[P_2Mo_{18}O_{62}] \cdot 4C_4H_8O_2 \cdot 16H_2O$ after thermal treatment and rearrangement at 550°C for 4 h in air.

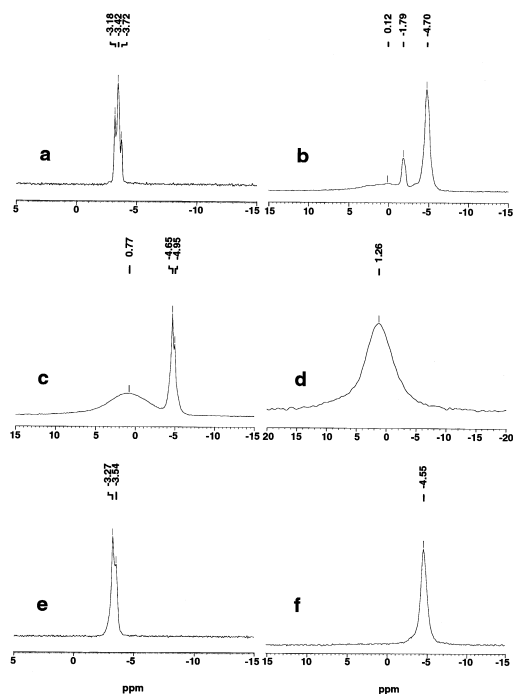


Fig. 8. Solid-state ^{31}P NMR spectra of $K_6[P_2Mo_{18}O_{62}] \cdot 4C_4H_8O_2 \cdot 16H_2O$: (a) at room temperature, (b) and (c) after heating to 300 and 550°C for 6 h in air, respectively, (d) the product of the reaction between $K_3[PMo_{12}O_{40}]$ and K_3PO_4 in a 1:3 mole ratio; and of $(NH_4)_6[P_2Mo_{18}O_{62}] \cdot 4C_4H_8O_2 \cdot 8H_2O$: (e) at room temperature, (f) after heating to 300°C for 6 h in air.

further information. For both $K_6[P_2Mo_{18}O_{62}] \cdot 4C_4H_8O_2 \cdot 16H_2O$ and $(NH_4)_6[P_2Mo_{18}O_{62}] \cdot 4C_4H_8O_2 \cdot 8H_2O$ the spectra (Fig. 8a and e, respectively) reveal several signals in each case [K^+ salt: -3.18 , -3.42 and -3.72 ppm; NH_4^+ salt: -3.27 , -3.54 and a shoulder at ~ -2.9 ppm]. This indicates the presence of several compounds in each solid sample, although solution studies showed the presence of only one species in both cases. These separate signals presumably arise from loss of water and/or dioxane from the originally precipitated materials to produce separate compounds, as indicated above. Although it is possible that separate signals could arise from two unique phosphorus atoms within a single $[P_2Mo_{18}O_{62}]^{6-}$ ion (or indeed within a unit cell), this would lead to signals of identical intensity, which is not ob-

served. On heating to 300°C in air for 6 h, the spectrum of $K_6[P_2Mo_{18}O_{62}]$ (Fig. 8b) exhibited a major resonance at -4.70 ppm, which is attributed to $K_3[PMo_{12}O_{40}]$ [24], a second smaller resonance at -1.79 ppm and a weak but very broad signal centred at ~ 0.12 ppm. The presence of at least two components at this temperature is consistent with the TEM study (Fig. 6c). At 550°C (Fig. 8c), the signal at -1.79 disappeared, while the broad resonance increased and was now centred at 0.77 ppm, while there were two signals at -4.65 and -4.95 ppm, which can be attributed to $[PMo_{12}O_{40}]^{3-}$ -containing compounds. The broad signal at 0.77 ppm may be compared with that of the product of the reaction of $K_3[PMo_{12}O_{40}]$ and K_3PO_4 in a 1:3 mole ratio, which gave a broad signal at 1.26 ppm (Fig. 8d). Although not quite at the same chemical shift, the broad signal, partially observable at 300°C after 6 h and fully formed at 550°C in the spectra resulting from thermal treatment of $K_6[P_2Mo_{18}O_{62}]$, may be attributed to the amorphous component observed in the SEM study (Fig. 7). For $(NH_4)_6[P_2Mo_{18}O_{62}]$ on heating to 300°C in air for 6 h the spectrum was much simpler (Fig. 8f), with only one component observable at -4.55 ppm, which can be attributed to $(NH_4)_3[PMo_{12}O_{40}]$ [24]. The second component presumably either occurs at the same chemical shift (there is a shoulder at ~ -3.0 ppm) or perhaps may have volatilised from the sample.

3.2. Oxidative dehydrogenation of isobutyraldehyde — catalysis by salts of the Dawson ion $[P_2Mo_{18}O_{62}]^{6-}$

The data for the oxidative dehydrogenation of isobutyraldehyde by the K^+ , NH_4^+ and Me_4N^+ salts of the $[P_2Mo_{18}O_{62}]^{6-}$ ion are given in Table 1. In all cases the conversion is relatively low ($< 30\%$) and is, interestingly, lower at the higher temperature. The main products (with the exception of the K^+ salt at 250°C) are acetone and CO_2 , the latter particularly at the higher temperature. The increased formation of CO_2 at 250°C probably stems from increased oxidation of the product species with increasing temperature, as the CO selectivity changes little or is even smaller as the temperature is raised. The reduction in conversion at 250°C is surprising, as increases in temperature over the range 225–350°C generally lead to increases in conversion for the related Keggin-type structures in this and other oxidative dehydrogenation reactions [1,22]. Moreover, the thermal stability studies described above indicated that the $[P_2Mo_{18}O_{62}]^{6-}$ ion should have been stable over the time required for the catalysis studies. In terms of the electrochemical reduction potential (determined by cyclic voltammetry at a glassy carbon electrode in a 50:50 v/v 0.5 M H_2SO_4 – H_2O :1,4-dioxane solution) for the $[P_2Mo_{18}O_{62}]^{6-}$ and $[PMo_{12}O_{40}]^{3-}$ ions, the most positive 2-electron reversible $E_{1/2}$ potentials occur at $+0.338$ and $+0.177$ V (vs. Ag/AgCl), re-

Table 1
Catalytic dehydrogenation of isobutyraldehyde using K^+ , NH_4^+ and Me_4N^+ salts of $[P_2Mo_{18}O_{62}]^{6-}$

Catalyst	Temperature (°C)	% Conversion	% Selectivity ^a			
			MAL	ACE	CO	CO ₂
$K_6P_2Mo_{18}O_{62}$	225 ^b	29	7	66	16	11
	250 ^b	27	37	34	8	21
$(NH_4)_6P_2Mo_{18}O_{62}$	225 ^b	21	14	46	12	28
	250 ^b	16	6	32	13	49
$(Me_4N)_6P_2Mo_{18}O_{62}$	225 ^b	22	8	59	9	24
	250 ^b	4	7	49	9	35

^a MAL, methacrolein; ACE, acetone.

^b Calcination temperature = 255°C for 2 h under a flow of nitrogen + 3% oxygen.

spectively, indicating that the Dawson anion is a slightly stronger oxidant. Moreover, the HOMO-LUMO gap for the anions are 4.83 and 4.79 eV, respectively (EHMO calculations), suggesting only a slight difference in the energies required to reduce these anions and, hence, a similarity in their relative oxidizing abilities. Any differences in catalytic activity over the temperature range studied are, therefore, likely the result of structural instability. Indeed, examination of the IR spectra of the spent catalysts did indicate substantial thermal rearrangement, unexpectedly showing less thermal rearrangement of the K^+ salt than the NH_4^+ and Me_4N^+ salts under the conditions employed in the catalysis. This is, however, consistent with the increased selectivity towards methacrolein formation at 250°C that is exhibited by the K^+ salt. This cannot be the result of surface area differences, as the respective surface areas of the K^+ , NH_4^+ and Me_4N^+ salts of the $[P_2Mo_{18}O_{62}]^{6-}$ ion were 1.0, 1.5 and 1.2 m²/g, respectively.

The thermal rearrangement of the $[P_2Mo_{18}O_{62}]^{6-}$ ion under catalytic conditions as opposed to the static thermal stability studies described above likely stems from loss of rigidity of the anion through removal of a (lattice) oxygen atom. The conversion of isobutyraldehyde to methacrolein involves loss of two hydrogen atoms and it is likely that the mechanism of the reaction is similar to that of the oxidative dehydrogenation of isobutyric acid, which is bulk catalysis-type II [4,5,25]. In this case, following dehydrogenation of the substrate, this process involves the transfer of two H^+ ions and two electrons to the catalyst bulk, followed by formation of water through the loss of an anion (lattice) oxygen. In the case of $[P_2Mo_{18}O_{62}]^{6-}$, there are several types of oxygen atoms that could be involved in this process. For the reaction [Eq. (2)]:



the change in total stabilization energy ΔE_T for each of the potential oxygen atom positions

varies from +12.2 to +13.3 eV (per $[P_2Mo_{18}O_{62}]^{6-}$) for the terminal and bridging (i.e., 2-coordinate) oxygen atoms, and ca. +7.8 eV for the internal 3- and 4-coordinate oxygen atoms (those forming the oxygen atom environments of the phosphorus atoms). However, the latter are internal rather than surface atoms and will not be involved in this process. Thus, the change in total stabilization energy ΔE_T (~ 13 eV per $[P_2Mo_{18}O_{62}]^{6-}$) for the formation of water, an actual step in the mechanism, is greater than that required for thermal rearrangement, given by Eq. (1) (ca. +3.7 eV per $[P_2Mo_{18}O_{62}]^{6-}$) and is, moreover, also greater than that required for the de-dimerization of the $[P_2Mo_{18}O_{62}]^{6-}$ ion [Eq. (3)]:



which is +5.3 eV (per $[P_2Mo_{18}O_{62}]^{6-}$). This latter reaction is a plausible first stage in any thermal rearrangement of the $[P_2Mo_{18}O_{62}]^{6-}$ ion. It is therefore, likely that at the temperatures operating in the catalytic dehydrogenation of isobutyraldehyde (225 and 250°C), the loss of a lattice oxygen is sufficient to decrease the rigidity of the resulting $[P_2Mo_{18}O_{61}]^{6-}$ ion and lead to structural rearrangement. Moreover, as the ratio of the number of moles of isobutyraldehyde introduced in 4 1/2 h (4 h required to reach a steady state plus ca. 1/2 h sampling) per mole of catalyst is ca. 100:1, over this time period it is possible for every anion to be involved in the reaction leading to a substantial fraction undergoing rearrangement. The decrease in activity at the higher temperature, therefore, supports an oxidative dehydrogenation reaction for isobutyraldehyde in which an anion (lattice) oxygen is involved in the overall mechanism.

The above results also suggest that the nature of the cation is important in stabilizing the Dawson structure under catalytic conditions. This is probably related to the relative charge densities of K^+ vs. both the NH_4^+ and Me_4N^+ cations and their ability to restrict movement of

electron-rich decomposition fragments. However, the thermal rearrangement of the Dawson structure above $\sim 260^\circ\text{C}$ precludes any investigation and comparison with related salts of $[\text{PMo}_{12}\text{O}_{40}]^{3-}$ under increased temperature conditions that are more favourable to the selectivity of methacrolein.

3.3. Oxidative dehydrogenation of isobutyraldehyde — catalysis by the thermally-rearranged Dawson phases

Above $\sim 260^\circ\text{C}$, the $[\text{P}_2\text{Mo}_{18}\text{O}_{62}]^{6-}$ ion thermally rearranges into $[\text{PMo}_{12}\text{O}_{40}]^{3-}$ and a second (or more) product(s), the nature of which depends on the cation, as discussed above. The catalysis results (at 275 and 300°C) for the oxidative dehydrogenation of isobutyraldehyde using a range of thermally-rearranged $[\text{P}_2\text{Mo}_{18}\text{O}_{62}]^{6-}$ phases following calcination at 310°C are given in Table 2. The results for the the K^+ , Rb^+ and Cs^+ -containing phases are similar. In each case, the conversion is relatively low ($< 18\%$ maximum), with the favoured

products being acetone, CO and CO_2 , with increases in the latter at 300°C . This is again presumably because of increased oxidation of the product species at the higher temperature. The maximum selectivity towards methacrolein is only 9%. However, the results for the NH_4^+ - and Me_4N^+ -containing phases are significantly different. Although the conversions are only modest at 275°C , the selectivity to methacrolein is considerably higher, 52 and 76% for the NH_4^+ - and Me_4N^+ -containing phases, respectively. At 300°C , the conversions are even greater (80–90%) while the combined selectivities to methacrolein and its oxidation product, methacrylic acid, are 73 and 77%, for the NH_4^+ - and Me_4N^+ -containing phases (with 2 and 10% methacrylic acid, respectively). In general, previous studies have reported that somewhat larger W/F values (and hence, residence times) are required to oxidize methacrolein to methacrylic acid at 300°C than encountered in this study (~ 0.4 – 3.6 vs. 0.2 g s/ml in the present study [2]). Also, the reported contact time for the industrial oxidation of methacrolein to metha-

Table 2

Catalytic dehydrogenation of isobutyraldehyde using thermally-rearranged $[\text{P}_2\text{Mo}_{18}\text{O}_{62}]^{6-}$ phases and pure $(\text{C}^+)_3[\text{PMo}_{12}\text{O}_{40}]$ ($\text{C}^+ = \text{K}^+$, NH_4^+ and Me_4N^+) phases after calcination at 310°C (nitrogen + 3% oxygen)

Catalyst ^a	Temperature ($^\circ\text{C}$)	% Conversion	% Selectivity ^b				
			MAL	MAA	ACE	CO	CO_2
$\text{K}_6\text{P}_2\text{Mo}_{18}\text{O}_{62}$	275	2	8	–	57	13	22
	300	3	5	–	43	11	41
$\text{Rb}_6\text{P}_2\text{Mo}_{18}\text{O}_{62}$	275	18	9	–	13	36	42
	300	12	3	–	11	33	53
$\text{Cs}_6\text{P}_2\text{Mo}_{18}\text{O}_{62}$	275	11	7	–	58	17	18
	300	12	6	–	50	17	27
$(\text{NH}_4)_6\text{P}_2\text{Mo}_{18}\text{O}_{62}$	275	15	52	–	6	37	5
	300	83	71	2	< 1	20	6
$(\text{Me}_4\text{N})_6\text{P}_2\text{Mo}_{18}\text{O}_{62}$	275	39	76	–	3	15	6
	300	90	67	10	< 1	14	9
$\text{K}_3\text{PMo}_{12}\text{O}_{40}$	275	36	58	< 1	5	27	10
	300	75	69	1	3	15	12
$(\text{NH}_4)_3\text{PMo}_{12}\text{O}_{40}$	275	61	71	< 1	6	12	10
	300	81	62	2	5	17	13
$(\text{Me}_4\text{N})_3\text{PMo}_{12}\text{O}_{40}$	275	95	74	3	1	13	9
	300	~ 100	50	10	1	23	16

^a W/F for the thermally-rearranged Dawson phases is 0.2 g s/ml and for the Keggin phases is 0.08 g s/ml.

^bMAL, methacrolein; MAA, methacrylic acid; ACE, acetone.

rylic acid, using a modified heteropoly catalyst system, varies from 2 to 6 s (0.14 s in the present study) over the temperature range 270–350°C [4,5]. This indicates that the thermally-rearranged Dawson phases with NH_4^+ and Me_4N^+ counter cations are active catalysts in these types of oxidative dehydrogenation and oxidation reactions.

The low conversions and low selectivities observed for the K^+ , Rb^+ and Cs^+ -containing phases probably result from poor crystallinity and hence, surface disorder, and/or to the presence of the second phase(s). The latter likely covers or partially covers the surfaces of the crystals of the Keggin structure phases $(\text{C}^+)_3\text{[PMo}_{12}\text{O}_{40}]$ (where $\text{C}^+ = \text{K}^+, \text{Rb}^+, \text{Cs}^+$). Evidence for this was presented above. In general, the free acid and salts of the $[\text{PMo}_{12}\text{O}_{40}]^{3-}$ ion are active catalysts in the oxidative dehydrogenation of isobutyraldehyde [10,11,22]. Data for $\text{K}_3[\text{PMo}_{12}\text{O}_{40}]$ are included in Table 2. Not only is pure $\text{K}_3[\text{PMo}_{12}\text{O}_{40}]$ more active than thermally-rearranged $\text{K}_6[\text{P}_2\text{Mo}_{18}\text{O}_{62}]$, but this is further emphasised given the W/F values employed in the two studies. The conversion and selectivities of the thermally-rearranged phase are slightly improved by calcination at 550°C, as shown for the K^+ -containing phase in Table 3. This cannot be attributable to surface area effects as the surface areas of the thermally-rearranged phases that are produced after calcination of $\text{K}_6[\text{P}_2\text{Mo}_{18}\text{O}_{62}]$ at 310 and 550°C for 4 h are 2.4 and $\sim 0.1 \text{ m}^2/\text{g}$, respectively. Some increases in conversion of the material calcined

at 550°C are noted and, while acetone is still the major product, some formation of methacrylic acid does occur at 300°C. The increased performance at 550°C is attributable to the considerably more crystalline nature of the phase compared to the material calcined at 310°C, as shown by the TEM and SEM studies. However, the overall relatively poor performance of this material can be attributed to the surface layer of amorphous material covering large sectors of the $\text{K}_3[\text{PMo}_{12}\text{O}_{40}]$ crystals as shown in the SEM study, which also contributes to the very low surface area of the material.

For the NH_4^+ - and Me_4N^+ -containing phases, the presence of a second phase does not seem to have the same effect in reducing the catalytic ability of the corresponding Keggin-based structures. Again, this cannot be attributable to any changes in the surface areas of the phases, as these were 1.5 and $1.2 \text{ m}^2/\text{g}$ for the NH_4^+ and Me_4N^+ salts of the $[\text{P}_2\text{Mo}_{18}\text{O}_{62}]^{6-}$ ion prior to thermal rearrangement and 1.4 and $1.5 \text{ m}^2/\text{g}$ for the respective NH_4^+ - and Me_4N^+ -containing phases following thermal treatment. It is suggested that under the conditions of thermal rearrangement of $[\text{P}_2\text{Mo}_{18}\text{O}_{62}]^{6-}$, the formation of analogous phases with NH_4^+ and Me_4N^+ counter cations to those formed in the K^+ , Rb^+ and Cs^+ systems does not occur, perhaps being thermally unstable themselves. In this regard, the ability of various *iso*- and *hetero*-polyoxometalates to be stabilized by different cations is well-established [6]. Lack of a well-defined second phase is also provided by the solid-state

Table 3
Catalytic dehydrogenation of isobutyraldehyde using $\text{K}_6\text{P}_2\text{Mo}_{18}\text{O}_{62}$ and thermally-rearranged phases after calcination of $\text{K}_6\text{P}_2\text{Mo}_{18}\text{O}_{62}$ at various temperatures

Calcination temperature (°C)	Catalysis temperature (°C)	% Conversion	% Selectivity ^a			
			MAL	ACE	CO	CO ₂
310	275	2	8	57	13	22
310	300	3	5	43	11	41
550 ^b	275	17	< 1	77	11	11
550 ^b	300	11	< 1 ^c	50	13	31

^a MAL, methacrolein; ACE, acetone.

^b Calcined in air for 4 h.

^c Five percent methacrylic acid also formed.

^{31}P NMR results described above. Comparison in these two cases with the corresponding pure Keggin salts, $(\text{NH}_4)_3[\text{PMo}_{12}\text{O}_{40}]$ and $(\text{Me}_4\text{N})_3[\text{PMo}_{12}\text{O}_{40}]$, is interesting, and the data are also given in Table 2. Both authentic Keggin-type catalysts are highly active at 275°C , unlike the thermally-rearranged phases formed from the corresponding Dawson structures, while at 300°C , the conversions are comparable or slightly better for the pure Keggin phases, even though their W/F values are smaller. This is likely associated with poor crystallinity for the initially-formed thermally-rearranged products which improves with time and increasing temperature, as is evident on comparing the data at the two temperatures. In contrast, the selectivities towards methacrolein and methacrylic acid are comparable for the thermally-rearranged Dawson and Keggin phases. Moreover, subsequent oxidation of the initially-formed product methacrolein to methacrylic acid is a surface-governed reaction with the rate of reaction proportional to the surface area of the catalyst [25]. The results for the thermally-rearranged Dawson phases are encouraging given that the surface areas of the pure Keggin phases $(\text{NH}_4)_3[\text{PMo}_{12}\text{O}_{40}]$ and $(\text{Me}_4\text{N})_3[\text{PMo}_{12}\text{O}_{40}]$ were 120 and $4.0\text{ m}^2/\text{g}$, respectively. These are 86 and $\sim 3 \times$ greater than those of their analogous thermally-rearranged phases, although it should be appreciated that in each case, the extent of subsequent conversion of methacrolein to methacrylic acid was low at the W/F values examined. Comparison of the present data with that of previously reported data [9–11] for the oxidative dehydrogenation of isobutyraldehyde to methacrolein suggests that the thermally-rearranged phases containing NH_4^+ and Me_4N^+ cations are highly active in this reaction.

4. Conclusions

Alkali metal, ammonium and tetramethylammonium salts of the Dawson anion $[\text{P}_2\text{Mo}_{18}\text{O}_{62}]^{6-}$ undergo thermal rearrangement at tem-

peratures greater than $\sim 260^\circ\text{C}$ to give the corresponding Keggin species $[\text{PMo}_{12}\text{O}_{40}]^{3-}$ and, in the case of the alkali metal salts, a second (or more) phase. The presence of this second phase is detrimental to the performance of the catalytically active Keggin phases. In the case of the NH_4^+ and Me_4N^+ salts, the second phase does not appear as thermally stable and the resulting solids are highly active catalysts for the oxidative dehydrogenation of isobutyraldehyde. The Dawson anions themselves were shown to be poor catalysts, undergoing structural breakdown during actual catalysis, likely because of the loss of lattice oxygen.

Acknowledgements

The authors would like to acknowledge Mr. M. Littlefair, of B.H.P. (Newcastle Laboratories) for performing the surface area measurements, Ms. C. Allen and Mr. K. Grice for help in obtaining the structural data, Mr. G. Weber and Mr. D. Phelan, of the University Microscopy Unit, for recording the transmission electron microscopy and scanning electron microscopy images, and Dr. J. Hook of U.N.S.W. for obtaining the ^{31}P solid-state NMR spectra. Mr. J. Hu would also like to acknowledge the University of Newcastle for the award of a UNRS and an OPRS.

References

- [1] M. Akimoto, Y. Tsuchida, K. Sato, E. Echigoya, *J. Catal.* 72 (1981) 83.
- [2] Y. Konishi, K. Sakata, M. Misono, Y. Yoneda, *J. Catal.* 77 (1982) 169.
- [3] M. Misono, in: M.T. Pope, A. Müller (Eds.), *Polyoxometalates: From Platonic Solids to Anti-Retroviral Activity*, Kluwer, Dordrecht, 1994, p. 255.
- [4] M. Misono, *Catal. Rev.-Sci. Eng.* 29 (1987) 269.
- [5] M. Misono, *Catal. Rev.-Sci. Eng.* 30 (1988) 339.
- [6] M.T. Pope, *Heteropoly and Isopoly Oxometalates*, Springer, Berlin, 1983.
- [7] F. Cavani, C. Comuzzi, G. Dolcetti, E. Etienne, R.G. Finke, G. Sella, F. Trifirò, A. Trovarelli, *J. Catal.* 160 (1996) 317.

- [8] C. Comuzzi, G. Dolcetti, A. Trovarelli, F. Cavani, F. Trifirò, J. Llorca, R.G. Finke, *Catal. Lett.* 36 (1996) 75.
- [9] E. Muneyama, A. Kunishige, K. Ohdan, M. Ai, *J. Mol. Catal.* 89 (1994) 371.
- [10] K. Ishimi (Nippon Kayaku), *Japan Kokai* 50,149,611 (1975).
- [11] N. Ando (Japan Synthetic Rubber), *Japan Kokai* 53,124,211 (1978).
- [12] G.A. Tsigdinos, PhD Thesis, Boston University, 1961.
- [13] J.F. Garvey, M.T. Pope, *Inorg. Chem.* 17 (1978) 1115.
- [14] G.A. Tsigdinos, C.J. Hallada, *J. Less-Common Met.* 36 (1974) 79.
- [15] C. Rocchiccioli-Deltcheff, R. Thouvenot, R. Franck, *Spectrochim. Acta A* 32 (1976) 587.
- [16] R. Massart, R. Contant, J.M. Fruchart, J.P. Ciabrini, M. Fournier, *Inorg. Chem.* 16 (1977) 2916.
- [17] C. Mealli, D.M. Proserpio, *J. Chem. Educ.* 67 (1990) 399.
- [18] R. Strandberg, *Acta Chem. Scand. A* 29 (1975) 350.
- [19] R. Strandberg, *Acta Chem. Scand. A* 29 (1975) 359.
- [20] R. Allmann, *Acta Chem. Scand. A* 30 (1976) 152.
- [21] R.D. Shannon, C. Calvo, *J. Solid State Chem.* 6 (1973) 538.
- [22] J. Hu, R.C. Burns, in preparation.
- [23] M.T. Pope, *Inorg. Chem.* 11 (1972) 1973.
- [24] J.B. Black, N.J. Clayden, L. Griffiths, J.D. Scott, *J. Chem. Soc., Dalton Trans.* (1984) 2765.
- [25] T. Komaya, M. Misono, *Chem. Lett.* (1983) 1177.